MEASUREMENTS OF THE COMPLEX CONDUCTIVITY OF VACUUM VESSELS AT THZ FREQUENCIES

D. J. Scott[#,*], S. Jamison*, ASTeC, STFC Daresbury Laboratory, Warrington, UK,
P. J. Phillips*, University of Dundee Division of Electronic Engineering and Physics, UK,
I. R. R. Shinton[*], Physics and Astronomy, University of Manchester, Oxford Road, Manchester, UK,
*Also at the Cockcroft Institute, Daresbury Science and Innovation Campus, Warrington, UK

Abstract

Accurate determination of the wakefield effects for high intensity, short electron bunches is an area of active research in accelerator design. Of particular interest is the resistive wall wakefield which depends upon the complex conductivity of the vacuum vessel. This conductivity depends on factors such as the frequency of the applied field, the temperature of the vessel and the level of impurities in the vessel material and so is generally difficult to characterise for real vessels. An experiment for determining the complex conductivity properties of a cylindrical vessel at frequencies in the THz regime, through the sub-picosecond time-resolved measurement of pulsed THz radiation transmitted through the structure is presented.

INTRODUCTION

The calculation of resistive wall wakefields requires knowledge of the conductivity properties of metals. For bunches with structures ~10 microns, such as those found in the LCLS, the effects of an ac conductivity need to be considered [1]. In ac conductivity the field changes with a time period less than the mean time between collisions of conduction electrons, τ. Typical values for τ are 27 fs for copper, 2.3 fs for aluminium and 0.14 fs for stainless steel, where the value for stainless steel has been derived by considering the level of impurities [2, 3]. The ac conductivity is determined by the plasma frequency and τ, and the plasma oscillations are also of the order of ps to fs time scales. Therefore the frequencies associated with short bunch structures are of the order of THz which is also approaching the τ and plasma frequency of the conduction electrons in standard vacuum vessel materials.

Typically wakefield effects scale as an inverse power of the vessel radius and so a larger aperture vessel can be used to mitigate any deleterious effects. However in magnet designs requiring a high on-axis field a small vessel aperture is desired. Many wakefield effects, such as the amount of resistive wall heating are crucial for the design of superconducting magnets. Recent studies of superconducting undulators for light sources concluded that the amount of resistive wall heating would be too great for conventional cryo-coolers [4, 5]. However, the conductivity of materials at low temperatures is strongly dependant on the levels of impurities and so an experiment to measure the actual conductivity of real vessels at the frequencies supplied by short electron bunches would be beneficial for the development of these superconducting magnets. The impedance effects of NEG coatings used to obtain good vacuum in narrow gap vessels is also not well understood. The techniques used in this paper could be extended to measure the impedance effects of a NEG coating on a vessel.

A conventional method of measuring the conductivity of metals is to measure the reflectivity of an incident wave at a particular frequency, the reflection coefficients being proportional to the conductivity [6]. Such experiments are notoriously difficult at THz frequencies as the signal is small compared to the noise. Also, it would seem difficult to measure an actual vessel that would be used at cryogenic temperatures.

In the following the status of a new scheme is presented that could enable the characterisation of the conductivity properties of a wide range of vessels of different sizes, materials and in principal, temperatures. The scheme relies on the time-resolved measurement of the attenuation of the electric field as it propagates in a mode (or summation of modes) along a vessel which acts as a waveguide. By considering vessels of different lengths the relative absorption and phase delay of each mode can, in principal, be measured (see Figure 1).

PROPAGATION OF WAVEGUIDE MODES

The propagation of electromagnetic fields along waveguides is treated in many areas [7, 8] and, for example, at THz frequencies here [9]. The fields are composed of an infinite set of orthogonal modes. The modes themselves are decomposed into TE and TM modes. Some example modes are given in Figure 5. Each mode is characterised by an index that is usually two integers describing the field pattern in each of the transverse directions. Mixed modes of TEM type will not be considered here.

In general the transverse electric field, $\boldsymbol{E}_\perp$, can be represented as an infinite series of mode functions, e_{1i} and e_{2i} where the subscript i identifies the mode being considered and 1 and 2 indentifies the transverse co-ordinate, and a propagation term, expressed as a function of ω, and the propagation constant γ:

$$E_{\perp} = \left\{e_{1i}, e_{2i}\right\} Exp\left[\, j\left(\omega t - \gamma z\right)\right]$$

The propagation constant is a complex quantity, γ=α+jβ, where α is known as the attenuation constant and β is the phase constant. the signal from one length waveguide to one longer by z scales as (see Figure 1):

[#] duncan.scott@stfc.ac.uk

$$\frac{E_{signal}}{E_{reference}} \sim e^{-j\gamma z}.$$

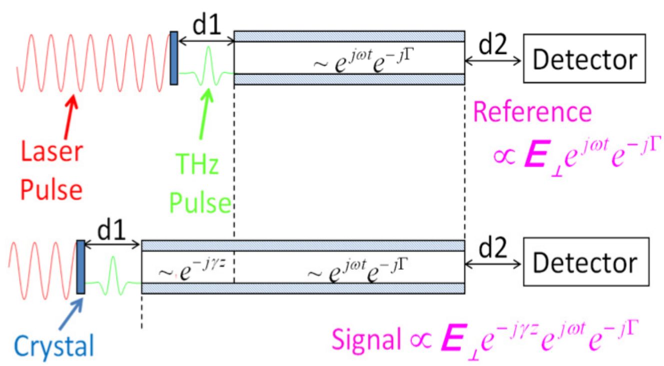

Figure 1: Scaling of propagation factors as the waveguide length is increased.

Example Attenuation

As an example of the amount of attenuation expected, Figure 2 shows the propagation of a THz pulse in the TE_{11} mode after passing through 50 cm of circular copper waveguide of diameters 5 and 2 mm with and without attenuation. The amount of attenuation is increased for smaller diameters or longer vessels.

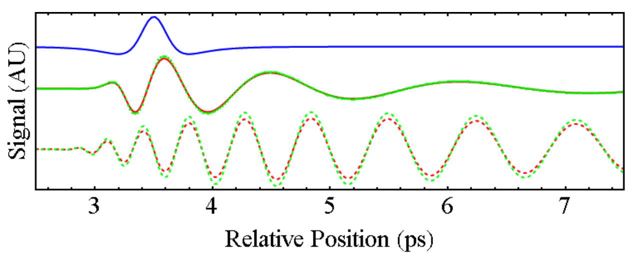

Figure 2: Propagation of a pulse (blue) through 50 cm of 5 mm (middle) and 2 mm (bottom) diameter waveguide with (red) and without (green) attenuation.

THE EXPERIMENTAL SET UP

Figure 3 gives an overview of the experimental set-up. A short (~40 fs) laser pulse from a high intensity Ti:Sapphire laser is split along two arms one known as the probe pulse the other as the pump. The pump beam passes through a ZnTe or GaP crystal generating a ~ps THz pulse, via optical rectification, which then passes through a vessel (waveguide). The end of the vessel (waveguide) provides the focus for a parabolic mirror (f=150 mm), which collimates the THz beam. There are beam blocks on the outside of the waveguide to insure that the THz detected is only that which passes through the waveguide. This THz beam is then incident onto a parabolic mirror (f=150 mm) to focus it onto the ZnTe detection crystal. The THz pulse and the probe pulse are set to be collinearly through the ZnTe crystal, being both spatially and temporally overlapped. The probe pulse is rotated by the THz pulse via interaction of the ZnTe crystal. Using a quarter wave plate and a beamsplitting polarizer together with a set of balanced photodiodes, the THz pulse amplitude is detected by monitoring the probe pulse polarization rotation after the ZnTe crystal at set delay times with respect to the THz pulse. Placing different length waveguides in the path of the THz pulse means that absorption changes due to the change in length can be measured (see Figure 1)

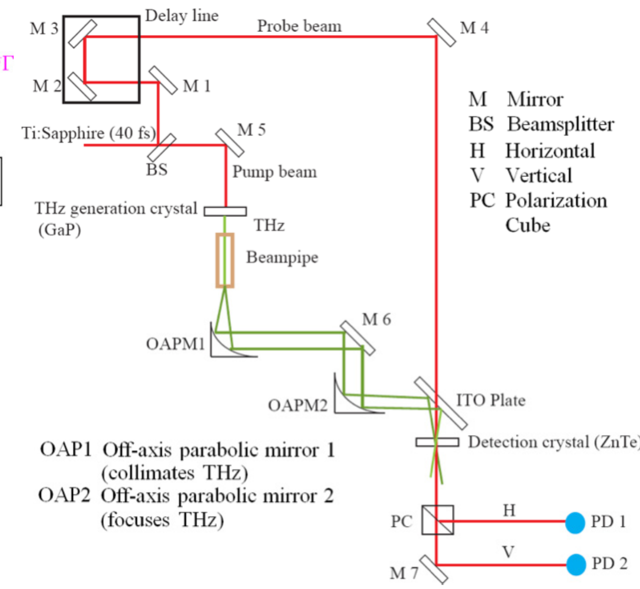

Figure 3: Experimental set-up.ayout of the text on the page is illustrated in Fig. 1.

INITIAL EXPERIMENTAL RESULTS

Figure 4 shows the initial experimental results obtained for a 5 mm copper circular waveguide 2.5 cm and 10 cm long. Also shown is the measured THz pulse with no waveguide present. The results were reproducible over three separate measurements (although the waveguide was kept in place for each data-set). After the initial pulse there is ringing due to the attenuation, water absorption and higher frequency terms as a GaP crystal was used for generating the THz and ZnTe for detection. The signal changes with length of waveguide and whether there is a waveguide present and the 10 cm waveguide show dispersion of the signal. It is planed to repeat the experiment with improved signal to noise, and longer and/or shorter diameter waveguides.

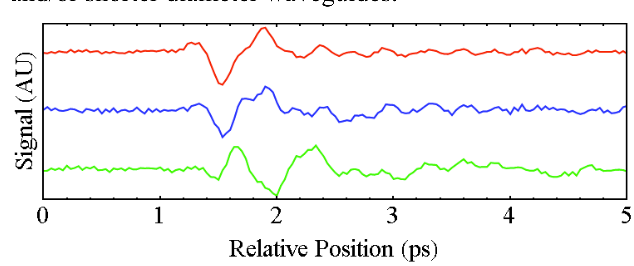

Figure 4: measured signal after the initial pulse (red) is propagated through 2.5 cm (blue) and 10 cm (green) 5 mm diameter copper waveguide.

MODE MATCHING

It is still to be determined which modes are excited by the incident laser pulse, and by what fraction. The technique of mode matching can be used. This has been developed for microwave engineering [10, 11] and is briefly explained here. At a junction of a waveguide there are reflections and so there are waves travelling in the positive and negative z directions. The amplitudes of the waves travelling in a each direction, A and B, can be obtained by projection of the transverse components of the incoming electromagnetic field pattern over the transverse field pattern of the modes (also known as the scalar product):

$$A_i + B_i = \int_{surf\ ace} \left(E_{in} . E_{out} \right) da$$

Mode Matching to the Incoming Laser Pulse

To a first approximation the initial laser pulse will have a constant field in the x direction. By inspection of the modes it can be seen that the coupling to the first few TM modes and the first few TE modes will be zero (see Figure 5). The lowest order mode that the field couples to is the TE11 mode. This was also found by calculation of the scalar product

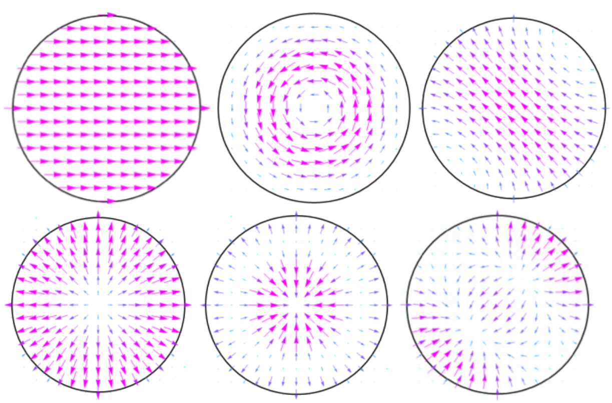

Figure 5: Electric field patterns for the incoming laser pulse, TE01, TE11, TM01, TM02 and TM11 modes.

Single Mode Propagation and Matching to a Step Junction

In a 5 mm diameter vessel many thousands of modes can propagate. This increases the complexity of the calculation. For waveguides of dimensions ~50 microns only one or a few modes would propagate. Using smaller geometries with fewer modes would simplify the mode matching analysis.

A simple geometry that should be easy to analyse is a single step junction between two circular waveguides of radius a and b. For example, the coupling from the TM0n to TM0m modes can be derived analytically and calculated numerically. Table 1 gives some values of A_i+B_i for different combinations of modes for a=30 and b=60 microns. Modes that are orthogonal have a scalar product of zero, as expected.

Table 1: example scalar products (analytical bold) at a step junction of two circular waveguides for a=30 and b=60 microns.

	TM_{01}	TM_{02}	TM_{11}	TM_{12}
TM_{01}	0.36 **0.36**	-0.054 **-0.053**	0	0
TM_{02}	-0.75 **-0.74**	0.059 **0.060**	0	0
TM_{11}	0	0	-0.015	0.26
TM_{12}	0	0	-0.81	-0.32

SUMMARY AND FUTHER WORK

In this paper the status of a new technique to measure the conductivity of metals via measuring the attenuation of the electric field when a THz pulse is transmitted through a waveguide has been presented. There are a number of theoretical and experimental areas that still need to be developed.

An initial experiment has been completed demonstrating the technique with a 10 and 2.5 cm, 5 mm diameter circular copper waveguide. This will be repeated with improvements to the signal and for longer and\or shorter diameter waveguides. The fabrication of some simple single mode waveguides of different lengths will be considered to help benchmark the theoretical analysis.

As well as the absorption part of the conductivity term in α there is also phase-dependant part. The time resolved nature of this experiments should allow this term to be investigated and that will be considered in further studies.

It may be possible to extend this technique to measure the conductivity properties of real vacuum vessels which will have applications in studying cryogenic vessels, vessels for short bunch lengths and studying the impedance effects of NEG coatings.

For the analytic studies a rigorous derivation of the propagation of waveguide modes with attenuation needs to completed and compared with the standard theory. Full mode matching of the waveguide modes to the initial laser pulse needs to completed to determine the most dominant modes and to calculate the expected propagation of the initial THz pulse.

REFERENCES

[1] K. L. F. Bane, SLAC-PUB-10707, SLAC, 2004
[2] D. J. Scott, EUROTeV-Report-2006-084
[3] Ashcroft & Mermin, "Solid State Physics"
[4] E. Wallen et al Cryogenics, 44, pp. 879–893, 2004.
[5] E. Wallen et al NIM A541, pg 630 2005
[6] Bane et al EPAC 2006, pp. 2955-2957
[7] D. M. Pozar "Microwave Engineering"
[8] N. Marcuvitz "Waveguide Handbook"
[9] T. Ito et al J. Opt. Soc. Am. B 24, pp.1230-1234, 2007
[10] J.C. Slater Rev Mod Phys 18 441-512, 1946
[11] J.C. Slater "Microwave Electronics"